

# Fourier Transform Infrared Spectrophotometer for Transmittance and Diffuse Reflectance Measurements

R. R. WILLEY

*Willey Corporation, Box 670, Melbourne, Florida 32901*

This paper describes a new Fourier transform infrared spectrophotometer with the capability to measure diffuse reflectance (DR) from 5000 to 500  $\text{cm}^{-1}$  (2 to 20  $\mu\text{m}$ ) in addition to the normal transmittance measurements. The instrument has a true simultaneous double beam measurement mode and a high speed single beam mode. The system also takes advantage of many data manipulation and display features due to the built-in computer and 2.5 million word storage system. One of the objectives of this work was to produce a practical instrument which includes the DR capability; another was to introduce the qualitative and quantitative measurements of DR in the infrared to the analytical community. DR has been commonly available in the visible and near ir spectrum, but until this new instrument, has not been available in the ir. A brief survey of the background and history of DR and emittance measurements in the ir is given. The design details and operation of the instrument are generally examined. Brief examples are provided for a few transmittance, trace analysis, and microsampling applications, and a variety of DR results are shown. The addition of diffuse reflectance as a tool in the infrared opens new avenues for investigation and application in many fields.

**Index Headings:** Infrared spectrophotometry; Double beam Fourier spectrophotometry; Diffuse reflectance, ir; Microsampling; Computer spectrum manipulation; Radiative transfer; Infrared spectra of solids.

## INTRODUCTION

We describe herein a new infrared spectrophotometer and a new measurement technique for the infrared, diffuse reflectance. The Willey 318S spectrophotometer is a Fourier transform instrument using a Michelson interferometer with all the normal ir functions and has the capability to measure diffuse reflectance in the 2 to 20  $\mu\text{m}$  spectral region. We provide some of the technical and historical background on the evolution of this tech-

nique and instrumentation, and set forth some examples of the early applications of the new measurement technique.

Since diffuse reflectance is a relatively new measurement in the infrared, we will first define our meaning. In specular or regular reflectance, the angle of incidence is equal to the angle of reflectance. In diffuse reflectance the direction of the reflected light is random with respect to the incoming beam. Fig. 1 illustrates specular and diffuse reflectance. Diffuse transmittance and regular transmittance have a similar relationship to diffuse and regular reflectance. Much work has been done in recent years on total internal reflection (TIR) or frustrated multiple internal reflection (FMIR) and the term "depth of penetration" has arisen.<sup>1</sup> In these cases the depth of the measurement or "penetration" is on the order of the wavelength. In the case of diffuse reflectance the depth of penetration is a function of the internal scattering of the material. Analogies of diffuse reflectance depths of penetration are a clear lake where one can see the bottom many feet below the surface and a muddy river where one can see only a few inches into the depth of the river. The total reflectance spectrum is due to the surface reflection plus the scattering and absorption of the particles in the medium. The general theory and practice of diffuse reflectance has been well documented by Frei and MacNeil.<sup>2</sup> They refer almost exclusively to work at shorter wavelengths in the visible and ultraviolet where diffuse reflectance has been commonly available from existing instrumentation. They describe in detail the parallel relationship to Beer's Law for transmission and the Kubelka-Munk Theory for reflectance from solids or powdered materials. They show that there are reasonable relationships

---

Received 24 December 1975; revision received 6 July 1976.

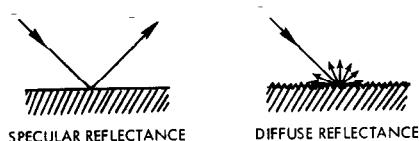


FIG. 1. Illustration of specular and diffuse reflectance.

for the concentration of various components in a mixture whereby one can determine quantitative information from diffuse reflectance of materials.

Diffuse reflectance spectrophotometry in the visible spectrum historically received a great boost by the work of Hardy<sup>3</sup> in the application of the first recording spectrophotometer in the 1930's. Hardy's primary work in the development and application of color measurement with integrating sphere technology provided the springboard for the development of this instrumentation in the new spectral region. Early work on the reflectance of materials was done by Coblenz in 1905 to 1908.<sup>4</sup> Hovis and Callahan<sup>5</sup> and Low<sup>6</sup> reported reflectance measurements on minerals. Various efforts have been made to provide special instrumentation for data which were needed in thermal radiative transfer problems as related to space technology; a survey of this work was reported by Dunn *et al.*<sup>7</sup>

Measurements of integrated reflectance or emittance without spectral information can be obtained by calorimetric and other techniques described elsewhere.<sup>8,9</sup> We will not discuss these here because of their limited interest to spectroscopists.

Many measurements of infrared reflectivity have been made to date by the technique whereby a sample is inserted into a blackbody cavity<sup>10</sup> and illuminated in all directions by the radiation from the blackbody's walls. The light reflected in a specific direction is compared with the light reflected and emitted from the sphere wall. The sample's temperature is controlled by water cooling so that effects of sample radiation can be accounted for in the measurement. This technique has limitations in that the sample must be cut to a specific size to fit the apparatus and inaccurate results may be obtained because of the lack of control of the sample's temperature if the sample is not a good thermal conductor. Further difficulties arise if the sample is affected by high radiation levels or high temperatures (burning, melting, or other changes).

Essentially the same measurement characteristics are achieved by ellipsoidal mirror techniques<sup>7</sup> which either illuminate the sample in all directions and examine it in a specific direction, or the reverse whereby the sample is illuminated in a single direction and all of the reflected radiation is collected and brought to a detector. The most satisfactory instrument of which we are aware prior to the development of the new instrument described in this paper was the Cary 90 with White reflectance attachment.<sup>11</sup> This attachment essentially falls in the category of a special case of ellipsoidal mirror and is often referred to as the Coblenz Hemisphere. All of the light emitted from a source into a hemisphere is reflected onto a sample and the sample is observed in a specific direction through a small hole in the specular reflecting hemisphere. The source and the sample essentially lie at two approximate foci of an ellipsoid. This

technique is, in effect, similar to a blackbody where the sample is irradiated in all directions by a source. Some of the limitations of sample size and cooling come into play in the case of this instrumentation also. Samples such as vegetation and paper-like materials can be difficult if not impossible to measure with any such instrumentation. Excellent and extensive results with the Cary 90 were obtained at the National Bureau of Standards by Keegan and Weidner.<sup>12</sup> A similar such instrument has resided at NASA Goddard Space Flight Center and been used by Hovis and Callahan.<sup>5</sup>

The geometry of the new instrument with its diffuse reflectance module is an integrating sphere related to that used in color measurement work in the visible spectrum. Typically, the sample is illuminated in a single direction and reflected energy in all directions is collected and integrated by the sphere whose interior surface is diffuse and highly reflective. As compared to the other alternatives, the amount of illumination of the sample is very small, corresponding approximately to the same flux level as received from a 100 W bulb at 1 m distance. The measurement times required to get full spectral data at moderate resolution with the new instrument are measured in seconds as opposed to the hours required by the other techniques. The speed of the new instrument is primarily due to the benefits of the Fourier transform technique in its application.

## I. INSTRUMENTAL DETAILS AND OPERATION

This instrument with the diffuse reflectance module, which will be discussed in more detail later, not only has the appropriate geometry to measure normal (or regular) transmittance, but also diffuse transmittance, normal (or specular, or regular) reflectance and diffuse reflectance.

Fig. 2 shows an optical layout of the instrument. The transmittance compartment is 12 cm wide with a beam separation of 10 cm and accommodates most of the usual transmittance attachments such as specular reflectance, microsampling, beam condenser, gas cells, GC-ir, FMIR, etc. Another feature in the transmittance compartment is a set of aperture pairs for 10, 3, 1,  $\frac{1}{3}$  mm, etc. Two equal apertures are machined in a sheet metal plate which slides into position just behind the sample holder, and the apertures are preregistered so each falls at the center of the sample and reference beams. This allows one to change the diameter of the sample beam used and simultaneously reduce the reference beam to maintain the 100% line. When the available sample is not as large as the normal 10 mm (round) beam, this proves convenient. Microsample work down to  $\frac{1}{3}$  mm diameter has been satisfactorily performed *without* the use of a beam condenser. Fig. 3 shows an example of a  $\frac{1}{3}$  mm sample of polystyrene. A laser beam identifies the center of the sample beam to assist in sample location.

When the diffuse reflectance module (integrating sphere) is in position, but only normal transmittance is required, a greater signal/noise ratio can be achieved by the use of an insertable optical device. This device reflects the transmitted beams directly onto the detector rather than allowing the energy to bounce around and

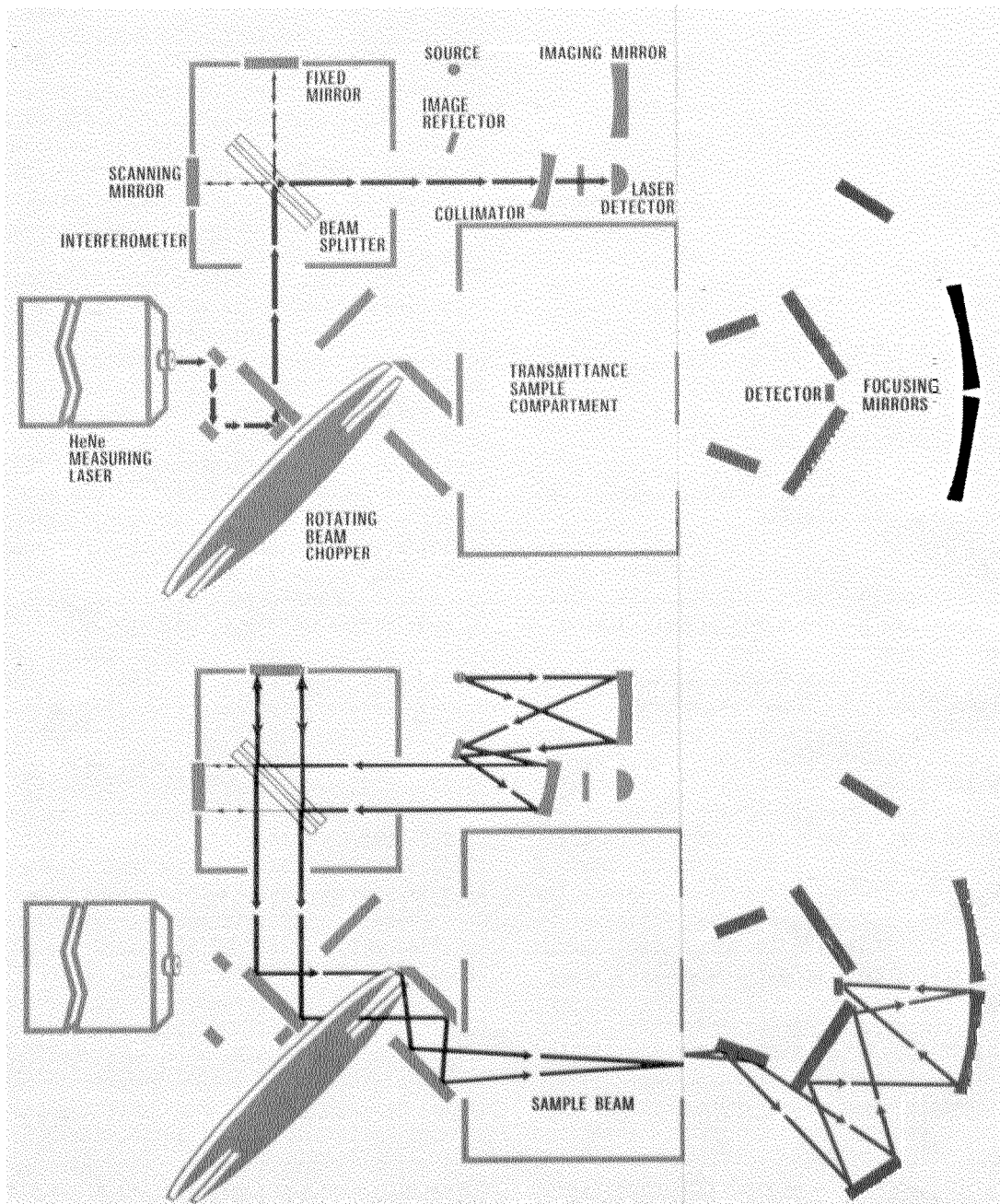


FIG. 2. Diagram of the Willey 319S interferometric spectrophotometer.

become diffused in the integrating sphere. The spectrum in Fig. 3 was obtained with the direct transmittance device in place. A  $4\times$  beam condenser has been used for samples as small as  $50\ \mu\text{m}$  in diameter.

The geometry of the integrating sphere in the diffuse reflectance module is shown in Fig. 4. The beam which focuses at the sample position in the transmittance compartment passes over the top of the integrating sphere and is redirected and focused downward by an off axis ellipsoid through the entrance hole in the sphere to the reflectance sample position at the bottom of the sphere. The image formed on the reflectance sample is approximately twice the size of the beam at the transmittance compartment; for example, the 10 mm aperture in the transmittance compartment is imaged at

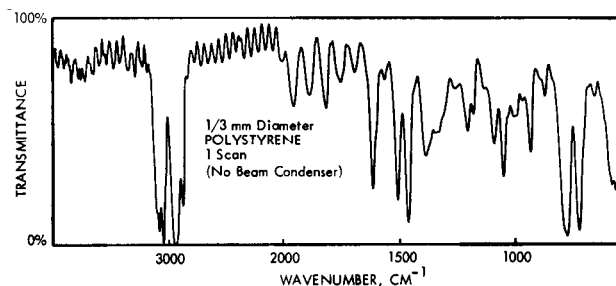


FIG. 3. Transmittance spectrum of a  $1/3$  mm diameter polystyrene film, single scan, without beam condenser,  $16\ \text{cm}^{-1}$  resolution.

about 20 mm diameter in the reflectance position, and the  $1/3$  mm aperture would be imaged at about  $2/3$  mm. The reflectance sample port is 25 mm in diameter.

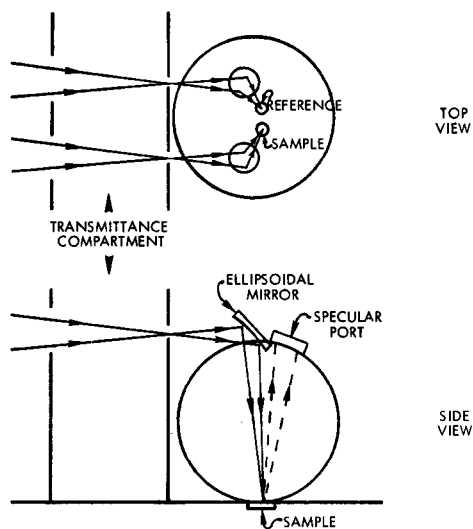


FIG. 4. Diagram of integrating sphere geometry ("DR" module) used for diffuse reflectance measurements.

The flux which is specularly reflected from a flat sample first intercepts the sphere wall at the top, and a specular port there can be opened by a knob which is external to the instrument to allow the specular (or gloss) component to be excluded from the measurement. The total reflected flux and diffuse component only can thus be measured and thereby the specular component can be derived from the difference. The specular component could also be measured with a specular reflectance attachment in the transmittance compartment.

Diffuse transmittance is accomplished by placing the sample over the entrance port to the sphere so that all the forward scattered and transmitted flux enters the sphere. The regular component of transmittance is included or excluded by covering the reflectance sample port with a "100%" reflector or not using the reflector, respectively.

Many of the elements of this Fourier transform spectrophotometer are the same as or equivalent to the elements of a conventional dispersive ir spectrophotometer. We will describe them in sequence along the optical and electronic paths with comparisons along the way. Descriptions of the optical elements refer to Fig. 2.

The source is a Nernst glower with platinum heater coils on an automatic starting circuit. The glower is shorter than those used in slit instruments; it is approximately square in the bright area and of about 2 mm diameter. The source imaging mirror focuses an image of the source onto an aperture of 3 mm which limits the angular extent of the beam when later collimated. An image reflector mirror behind this aperture directs the beam for convenience of space; the aperture is a field limiting stop. The emergent beam falls on the collimator mirror which is an off axis paraboloid and forms an image of the field stop at infinity. This beam enters the interferometer.

The spectral modulator is a Michelson interferometer which essentially causes different wavelengths or spectral frequencies to be modulated at different time frequencies. This is a major difference in detail from a conventional dispersive (prism or grating) monochromator that disperses a spectrum in angle and discrimi-

nates the wavelengths by position in space. The interferometer beamsplitter used here has a germanium coating on a KBr substrate. The interferometer has an adjustable compensator of equal thickness to the beamsplitter. The compensation can be adjusted to be exact by tilting the compensator plate to increase or decrease the optical path through it. This is generally not necessary since the software corrects for phase errors when performing the transform. The static mirror of the interferometer is adjustable for fine alignment of the interferometer optics. The interferometer is thermostated to minimize alignment changes due to environmental temperature changes. The elevated temperature of the interferometer also reduces the hazard of the KBr optics fogging due to humidity. Various moving mirror drives and suspensions have been used. The type currently used in the present system gives  $2 \text{ cm}^{-1}$  resolution. The moving mirror is suspended on a piston supported on metal diaphragms at two ends of the piston. Since the travel is relatively small, the diaphragms permit the piston to move freely along its axis, but prohibit any tilt of its axis (or the mirror). The linear motion drive is provided by a precision lapped leadscrew, turning in a compliant "Merton" nut which averages the screw errors over many threads. The screw was originally turned by a clock motor, but it was found that tooth to tooth gear errors and others limited the linearity of the drive. The current system has a precision toothless belt drive system which has been found to be much smoother. The subassemblies of the system are made in a modular fashion and allow easy maintenance and modification.

The motion of the interferometer mirror is monitored by a laser so that the exact position of the mirror determines when the interferograms are sampled. A HeNe laser beam is directed by mirrors through a small hole in the center of a fixed mirror in the ir channel. This beam then travels through the center of the interferometer in the opposite direction from the infrared beam so that it experiences exactly the same optical path as the ir beam. After leaving the interferometer, the beam passes through a small hole in the collimator mirror, through an interference filter to eliminate other wavelengths, and onto a silicon photodetector. The laser signal observed is a sine wave when the interferometer scans. The zero crossing points therefore represent 1 half-fringe ( $0.1582 \mu\text{m}$ ) of interferometer mirror movement. The present circuitry allows sampling of the ir interferograms to be triggered in any integral multiple of half-fringes up to 15. The sampling interval is normally 3 or 4 half-fringes.

The double beam or spatial modulation system in this instrument is unique for Fourier systems. The rotating beam chopper alternately directs the ir beam through the reference and sample channels with spaces between where neither channel is illuminated. This "zero" signal reference allows the amplitude of the signal in the reference and sample channels to be independently determined at each point for photometric accuracy. The chopper multiplexes the sample and reference channels in time and space; the rate is an order of magnitude higher than the highest frequency in the ir interferogram. The two channels travel equal optical paths and fall on the

same detector. The electronics amplify, demultiplex, and filter the signals such that two separate interferograms are simultaneously produced for the sample and reference channel. When the laser signals indicate that it is time to sample the interferograms for the next point, both interferograms are sampled simultaneously by sample and hold circuits. These are then converted from analog to digital values and stored in the computer. This process is repeated for the number of points to be gathered from the interferogram.

In the double beam mode, the interferometer scan is relatively slow as is dictated by the mechanical speed limitation of the double beam chopper. The single beam mode of the instrument can be used for greater speed. In the single beam mode, the double beam chopper is stopped at the channel desired, and the electronics switched to bypass the multiplexing. A different frequency response filter is used. The scan speed of the interferometer is changed by a mechanical speed shift button to 16 times the double beam speed. In the single beam mode,  $16\text{ cm}^{-1}$  resolution is obtained in 2 sec.

Some of the limitations of single beam operation are the same for Fourier as for dispersive instruments. Any changes in conditions from sample measurement time to reference measurement time appear in the spectrum. Examples are: atmospheric water vapor and  $\text{CO}_2$  changes in the instrument, source brightness changes, interferometer alignment, etc. Atmospheric effects can be bothersome at high resolution, but appropriate purging can reduce these to an acceptable level. The double beam mode eliminates this problem and the others.

In the diffuse reflectance (or diffuse transmittance) mode, all of the flux reflected (or transmitted) by a sample becomes evenly distributed over the inside of the integrating sphere wall which has an area of approximately  $1000\text{ cm}^2$ . This is opposed to a transmittance mode spectrophotometer where all the energy is concentrated on a detector of less than  $0.1\text{ cm}^2$ . This same area detector in the wall of the sphere will receive approximately  $10^{-4}$  of the total available flux as compared to a normal transmittance measurement. There is one factor which restores approximately 1 order of magnitude of signal. The light reflected from the sample reflects from the sphere wall diminished by the reflectance of the sphere wall, and this light reflects again from the sphere wall, etc. It can be shown<sup>13</sup> that the illumination on a highly reflective sphere wall is greater than it would be in a black sphere by a factor of  $r/(1-r)$ . Here  $r$  is the effective reflectance of the sphere wall accounting for hole losses, etc. This would give a factor of  $19\times$  "sphere gain" if the  $r = 0.95$ . The sphere surface should be as highly reflecting and diffuse (Lambertian) as practical for good signal and photometric accuracy. The current spheres are diffuse textured gold surfaces which reflect about 0.95 over the regions of interest.

The solution to the signal/noise ratio limitation of the integrating sphere is to use the advantages of multiplexing and throughput in the Fourier transform systems. This restores 1 to 2 orders of magnitude over a conventional dispersive system, to where reasonable results in diffuse reflectance can be obtained in typical ir spectrophotometer scan times of 2 to 30 minutes.

It can be shown that the signal/noise ratio at the

detector of this system is proportional to the  $D^*$  of the detector times the square root of the area of the detector. This is a somewhat unusual condition, and is due to the signal being a surface illumination which cannot be focused. Both pyroelectric and HgCdTe manufacturers were encouraged to provide as large an area detector as possible and still maintain the  $D^*$  so that the  $D^* \sqrt{A}$  would be maximized. The HgCdTe has proved best from  $2.5$  to  $18\ \mu\text{m}$  ( $4000$  to  $550\text{ cm}^{-1}$ ). The pyroelectrics seem to present strong microphonic difficulties in large areas.

When the signal/noise ratio (S/N) in a single scan is not as great as is desired, a multiple scan mode is available. As described extensively elsewhere,<sup>14</sup> the S/N can be increased generally as the  $\sqrt{N}$ , where  $N$  is the number of scans which differ only by random, independent noise. On numerous occasions, particularly difficult samples have been set up to scan repetitively overnight. Generally, thermal radiative transfer properties are quite satisfactory in a single scan. Maximum resolution single scan spectra usually show noticeable noise unless several scans are taken.

The spectral range of the instrument described is  $5000$  to  $500\text{ cm}^{-1}$ . The low frequency end is limited by the HgCdTe detector to  $450$  or  $500\text{ cm}^{-1}$ . With the pyroelectric, the limit is the KBr beamsplitter optics. A near ir version has also been constructed which operates from  $15\ 000$  to  $3000\text{ cm}^{-1}$  using a PbS detector. The range is limited by the detector, since the optics are fused silica. The rapid fall of the PbS at higher frequencies causes a more limited response above  $10\ 000\text{ cm}^{-1}$ .

The resolution is currently  $2\text{ cm}^{-1}$  which covers most applications. Higher resolution modules are in development at this time for gas phase work, etc.

The wavelength accuracy is unique in Fourier systems since it is tied to the HeNe laser. We have not yet performed rigorous tests, but the accuracy appears to be an order of magnitude better than the resolution.

The photometric accuracy in the double beam mode has been shown in preliminary tests to be better than 0.5% and primarily limited by S/N rather than by any other factor. Testing is not complete but indications are that 0.2% accuracy and precision are achievable and possibly 0.1%. The nature of the true double beam system and the slow scan allows the use of conventional sector wheels for calibration, but polished plates such as germanium, silicon, etc., of known index make good tests. The true double beam system is essentially the key to stability and reliability of the photometric scale.

The system described has incorporated in the hardware: a Modcomp II computer with GE Terminet, 1.3 or 2.6 M words of moving head disc storage, and 32 K core memory. The Terminet or a teletype is used for primary control of the instrument by the operator. The disc is used for semipermanent storage of spectra and other pertinent information and the core memory is part of the normal data processing.

The spectroscopist has the choice of processing the interferograms with apodizing<sup>15</sup> or not. The normal apodizing used is a triangular function which gives an instrumental line shape essentially like that of a diffraction limited grating instrument. The reference and sample interferograms are transformed with phase correction<sup>16</sup> applied to give two single beam spectra which

can then be displayed, ratioed, plotted, stored, taped, and otherwise processed. When transforms in excess of 1024 data points are used, the current software utilizes decimation<sup>17</sup> of the data into subsets which are stored on the computer's disc and processed sequentially rather than requiring excessive core storage in the computer.

Three spectrum output modes are used: console printout, chart plotter, or oscilloscope display.

The console printout mode is primarily tailored to the GE Termet where a spectrum is printed as a sequence of points where the horizontal scale on the paper is % $T$  or  $R$ , etc., and the vertical is frequency in wavenumbers or wavelength in micrometers. There are 3 spectral data points per print line. The scale can be plotted in percent, linear absorbance, or linear in the Kubelka-Munk function ( $F(R) = (1 - R)^2/2R$ ).<sup>2</sup> The latter function is linear in concentration for powder mixtures by reflectance, just as Beer's Law applies to liquid solutions. The values of  $T$  or  $R$  can also be listed by their respective wavelengths. The scale can be expanded by any value about the 100% or 0% line.

The plotter output used at present is a chart recorder. This plotter has no alphanumeric capability, but the wavenumber scale is well defined by fiducial marks generated at requested intervals (typically 500  $\text{cm}^{-1}$ ). The computer is programmed also to convert the normal display which is linear in wavenumbers to one which is linear in micrometers. This involves averaging points at the shortwave end and interpolating at the long wavelength end. Fiducials are displayed at every micrometer in this case. The plotter is calibrated for 0 and 100% scale, before plotting, by a control sequence which runs the pen to 100% for adjustment and the 0% on command.

The oscilloscope display output is built into the spectrophotometer and is connected to SYNC and vertical scale of an oscilloscope. The spectrum is displayed over any portion of the wavelength range and with any of the scales available in the other modes. One can request the single beam spectra from the sample and reference channels, and the ratio spectrum. One of the sense switches on the computer displays the 0 and 100% line on the scope for calibration. A variable low pass filter on the oscilloscope changes the spectrum's apparent slit width for smoothing. The scope display is convenient in terms of speed and flexibility, and it allows the spectroscopist to decide the best formats and scales before making a hard copy.

The disc system provides for storage of many spectra on the disc for later reference or further processing. The dual disc system utilizes an entire disc of 1.3 million 16-bit words to store spectra. This configuration stores over 600 high resolution spectra of 2048 points (2  $\text{cm}^{-1}$  resolution from 4000 to 400  $\text{cm}^{-1}$ ). Multiples of this number of spectra are obtained by inserting other disc cartridges. At current cartridge costs this represents \$.10 to \$.20 per spectrum for storage media.

A calibration program applies 100 and 0% ratio calibration spectra to a sample ratio spectrum and corrects for any departure in the 100 and 0% lines of the instrument. In the diffuse reflectance mode, a "100% curve" is usually run with a gold or aluminum mirror which could be independently calibrated on an absolute scale.<sup>18</sup> The "0% curve" is run by opening the sample

port and allowing the beam to escape. A light trap is usually positioned to prevent any of the escaping beam from being reflected back into the instrument. Room light is not a noticeable problem because it is not modulated in synchronization with the instrument choppers. Since these 0 and 100% lines do not change in the double beam mode over long periods of time, they are only run at the beginning and end of a day for photometric accuracy verification. They can then be applied to any or all of the spectra for the day.

The "difference" program subtracts one spectrum from another on a point-by-point basis after multiplying by whatever scale factor (concentration  $\times$  path length) is desired on the absorbance scale. This, then, treats the spectra in accord with Beer's Law. The program automatically computes the appropriate scale factor to null the difference in the two spectra at a specific wavenumber chosen by the spectroscopist and using a background region common in both spectra over a range specified by the spectroscopist. When the difference spectrum is displayed there is a null at the specified wavenumber. However, the spectroscopist may decide to null at another wavenumber or examine the influence of slightly greater or less subtraction ratios. These manipulations or changes are accomplished through console commands while examining the scope display.

Spectra can be summed together on a percentage scale also. The average of similar spectra can be found or the straight sum. This can be used to add the reflected and transmitted energy spectra of the sample to obtain the true absorbance spectrum.

A somewhat specialized program is available to compute the relative emissivity of a sample at a given temperature as compared to a blackbody. The reflectance spectrum of a sample if it is opaque, or the sum of  $R$  and  $T$  if transparent, is calibrated as desired and then the emittance spectrum is calculated;  $E(\sigma) = 1 - (R(\sigma) + T(\sigma))$ . This "curve" is then multiplied by the blackbody curve at the desired temperature and integrated over the spectral region desired and compared with the integrated blackbody curve to give the relative emittance of the sample to that of a blackbody at that temperature. This result is correct to the extent that the sample's absolute emittance is not actually a function of temperature at temperatures computed. These results agree well with other more difficult techniques of obtaining such data and have been particularly valuable in radiative transfer problems such as solar energy collectors and radiant heating panels.

## II. RESULTS

Since the purpose of this paper is to introduce the new measurement technique of diffuse reflectance in the ir, we do not attempt to report on any extensive research in various fields of application, but only to show a few examples of applications. We also will not comment at length on the chemical interpretation of the spectra since we are not presently expert in that field.

Figs. 3, 5, and 6 show a few conventional transmittance spectra for orientation of the reader who is accustomed to transmittance ir. Fig. 3 is a microsample of polystyrene (discussed above). Fig. 5 shows a typical

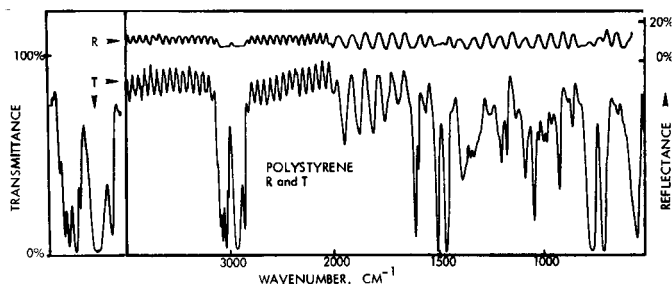


FIG. 5. Reflectance and transmittance spectrum of polystyrene film with expanded section of  $3000\text{ cm}^{-1}$  band at the left (not compressed  $2\times$  as is customary at frequencies higher than  $2000\text{ cm}^{-1}$ ).

polystyrene spectrum in transmittance. It will be noted that the scale is compressed  $2:1$  at frequencies above  $2000\text{ cm}^{-1}$  by averaging adjacent points (which reduces resolution in that region) to correspond to typical dispersive instrument spectra. The small section about  $3000\text{ cm}^{-1}$  is expanded  $2\times$  and shown at the left without compression to show the resolution. The reflectance spectrum of polystyrene is shown at the top of Fig. 5. The depth of the interference fringes is somewhat washed out in this reflectance spectrum due to varying film thickness over the  $25\text{ mm}$  sample. If a smaller sample beam in reflectance were used or a more uniform film thickness, the fringes in reflectance and transmittance should be complimentary where there are no significant absorptions. The physical characteristics of the reflectance spectrum are predominantly due to the index of refraction (Fresnel reflection) and interferences between the reflection from the front and back of the film.

Fig. 6A shows a section of a polystyrene spectrum of a sample which was measured before and after being smeared with Dow 704 silicone oil, wiped "clean," and then rerun. Fig. 6B shows the transmittance spectrum of the oil on a NaCl plate. The before spectrum was subtracted in the computer from the after spectrum and is shown without expansion ( $1\times$ ) and with  $40\times$  scale expansion in Fig. 6C. It can be seen that the before and after spectra were imperceptibly different when displayed as in Fig. 6A, but reasonably identifiable after subtraction and expansion. There is some residual effect of interference fringes in this difference spectrum; it appears that the before and after areas of the sample were not quite the same thickness (probably due to inexact registration). The area of each sample measured was  $1/3\text{ mm}$  in diameter.

The reflectance spectra of materials which are primarily diffuse are shown in the remaining figures. All of these spectra are plotted at  $8\text{ cm}^{-1}$  resolution except Figs. 14 and 16 which are at  $32\text{ cm}^{-1}$ . Typical scan times for the spectra shown are  $5\text{ min}$ .

Figs. 7 through 11 show organic materials which are primarily natural vegetable or animal in origin. Fig. 7 shows the reflectance spectrum of pure vegetable protein and starch which were provided by Dr. Karl Norris of USDA, ARS in Beltsville, MD. There are characteristic bands in protein at approximately  $1600$  and  $1700\text{ cm}^{-1}$  which can also be seen in the human hair and skin spectra of Fig. 8 and the spectrum of wool in Fig. 9. Fig. 8 also shows the transmittance spectrum of a dragon fly

wing which appears to have a protein-like spectrum. Human skin can be seen to be quite dark in this spectral region, and the characteristics from  $1500$  to  $2000\text{ cm}^{-1}$  seem to be mostly due to index of refraction changes around the absorption bands. These z-shaped changes in reflectance appear to have their maximum slope near the normal transmittance absorption maxima, and can probably be related to the physical theories of resonance. Most departures of DR spectra from transmittance spectra of the same materials that we have ob-

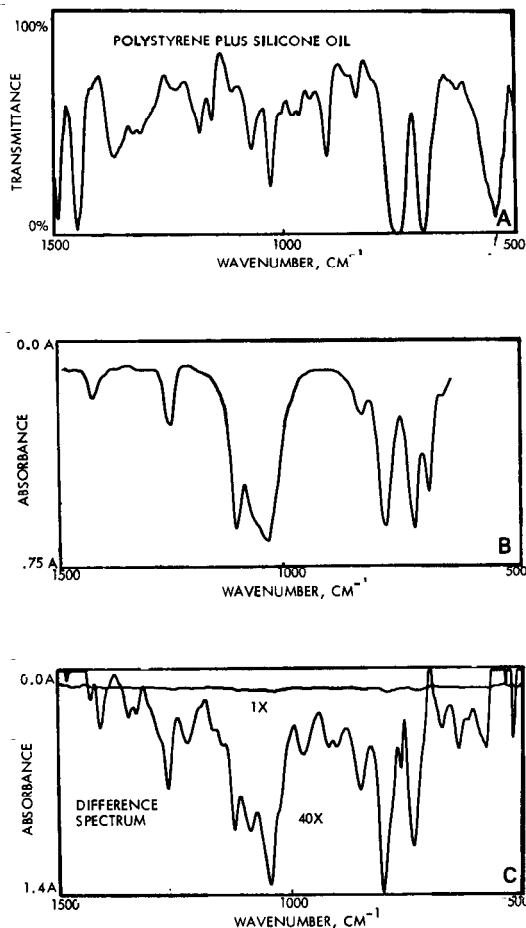


FIG. 6. A. Portion of normal transmittance spectrum of polystyrene film smeared with a trace of Dow 704 silicone oil at  $10\text{ cm}^{-1}$  resolution. B. DOW 704 silicone oil on NaCl plate at  $10\text{ cm}^{-1}$  resolution. C. Computed difference between spectrum of polystyrene film with silicon oil smear and film without smear shown above at  $1\times$  and below at  $40\times$  scale expansion. Resolution is  $10\text{ cm}^{-1}$  and shows silicon oil spectrum plus residual interference fringes.

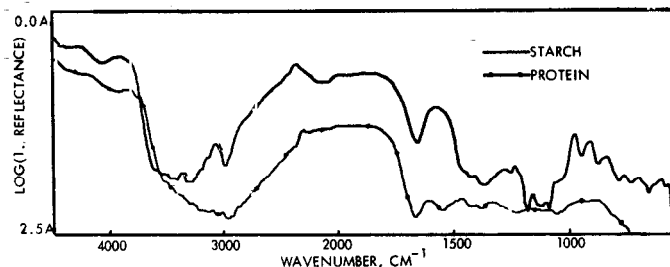


FIG. 7. Reflectance spectrum of vegetable starch shows characteristic bands at  $1600$  and  $3000\text{ cm}^{-1}$  and protein meal with dominant bands at  $1600$  and  $1700\text{ cm}^{-1}$ .

served seem to be of this nature, and generally the spectra are easily recognized.

In Figs. 9 and 10, the spectra of cotton, bond paper, and Kleenex are quite similar. We find many paper materials have similar spectra, and have been told that this is almost entirely cellulose.

Many leaves have been found to have generally low reflectance (below 10%) in most of this spectral range. Fig. 11 shows two examples. We have noticed a unique spectral signature in most of the plants that we have observed between 2900 and 3000  $\text{cm}^{-1}$ . This sharp pair of

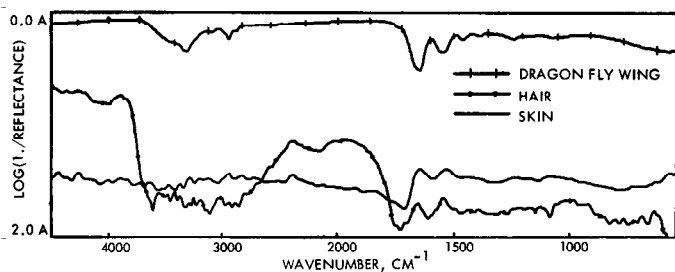


Fig. 8. Transmittance spectrum of dragon fly wing and reflectance spectra of human hair and skin showing correlations with protein bands.

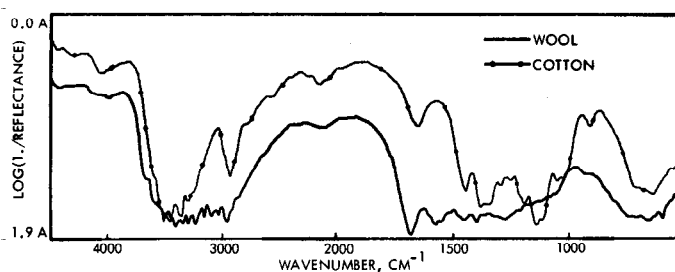


Fig. 9. Reflectance spectra of lamb's wool cloth and Red Cross cotton illustrating protein bands in wool at 1600 and 1700  $\text{cm}^{-1}$  and starch-like bands in cotton at 1600 and 3000  $\text{cm}^{-1}$ .

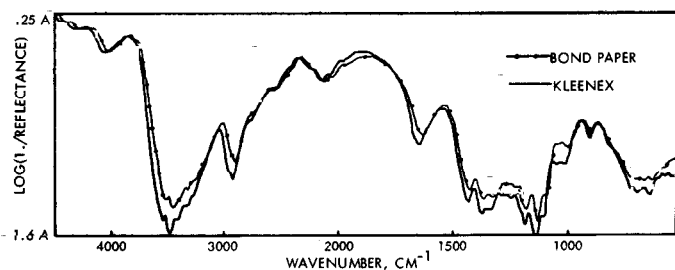


Fig. 10. Reflectance spectra of bond paper and Kleenex tissue showing similarities of the papers to each other and to cotton.

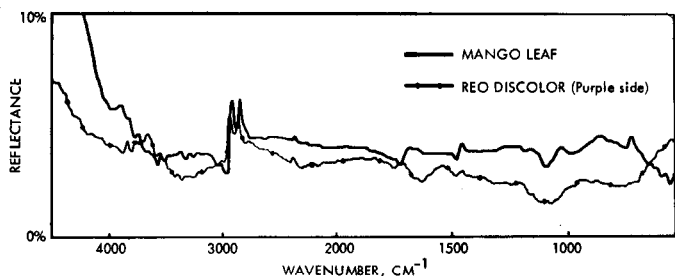


Fig. 11. Reflectance spectra of mango leaf and *Reo discolor* leaf (oyster plant) showing characteristic double peaks at 2900  $\text{cm}^{-1}$ . Change of index "z" bands are also seen at 700, 1100, 1500, and 1700  $\text{cm}^{-1}$  in mango leaf spectrum.

reflection peaks are anomalous dispersion effects around the two aliphatic C—H bands, according to P. R. Griffiths of Ohio University. The reflectance of the mango leaf shows several of the characteristic "z" bands mentioned above at 700, 1100, 1500, and 1700  $\text{cm}^{-1}$ .

Fig. 12 shows the great similarity between the reflectance spectra of Ivory and Lava soaps. It would appear that Lava is simply Ivory soap plus an additive (probably inorganic) material which generally reduces the reflectance but does not change the spectrum materially. Borax is shown here also because it produced a somewhat different spectrum. All soaps which we have measured show the dominant band at approximately 1600  $\text{cm}^{-1}$ .

Extensive work has been reported on the reflectance of minerals in recent years. Hovis and Callahan<sup>5</sup> with NASA and Aronson and Emslie<sup>19</sup> have done extensive work on experimental measurements and the development of theories which agree well with the results. Their investigations have shown the expected variation of reflectance spectra with particle size. Fig. 13 demonstrates these effects with a typical yellow sand. The reflectance spectrum of the sand was measured as collected. The same was then ground to particle sizes of approximately 1 order of magnitude smaller in a mortar and pestle before remeasurement. The smaller particle size material showed higher reflectance at higher frequencies and lower reflectance at lower frequencies as compared to the large particle sand. Similar relationships can be seen in Fig. 14 where a highly polished surface of limestone might be thought of as the ultimate in "large" particle size reflectance. The rough sawn sample of the same limestone shows the effect of the surface structure, and the reflectance spectrum of a sea shell shows the relationship of the shell to limestone. The limestone samples were provided by Querry who has done extensive work on specular reflectance.<sup>20</sup>

The calcium carbonate band from 1300 to 1500  $\text{cm}^{-1}$  seen in Fig. 14 is also apparent in the white roof coating in Fig. 15 which is a mixture of white lime and white portland cement. These white roof coatings are used to control the effects of solar heating in Florida and other places. It is desirable to have a white reflectance in the spectral region where the solar input is greatest (0.3 to 2  $\mu\text{m}$ ) to minimize the heat absorbed by the roof. It is further desirable to have as black a surface as possible in the infrared where blackbody radiation peaks for surfaces at 50 to 100°C. This maximizes the cooling due to thermal radiation from the surface. The spectra of Fig. 15 show that the infrared radiative properties of typical white cement roof tiles are all acceptable whether mildewed, clean, or white coated with the lime mix. However, the solar absorption properties do vary drastically. There is at least 1 order of magnitude more energy absorbed by the black mildewed tile than the white coated tile. This is found to have a real effect on air conditioning power consumption in residences and buildings. It can be readily seen that one would like just the opposite spectral characteristics in a "solar selective" absorber to gather solar energy. Here a black surface in the visible and "white" in the ir is desired to absorb as much sunlight as possible and not lose it by emission. Fig. 16 shows a black chrome solar selective

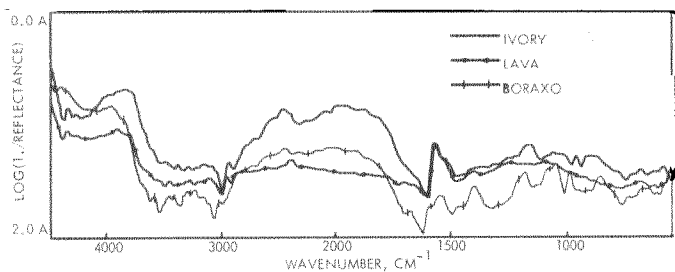


FIG. 12. Reflectance spectra of three soap products showing band at 1500 to 1600  $\text{cm}^{-1}$  and the close relationship of Ivory to Lava. Boraxo can be seen to have similar bands at 1000, 1600, and 3000  $\text{cm}^{-1}$ .

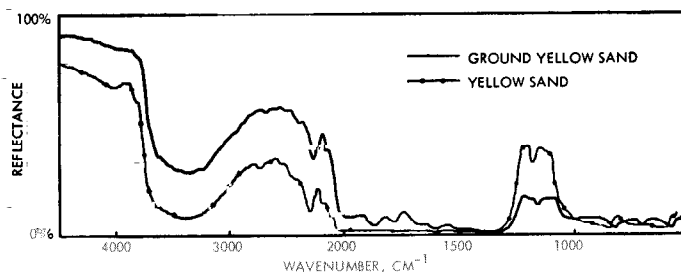


FIG. 13. Reflectance of local yellow sand at different particle size before and after grinding to particles an order of magnitude smaller.

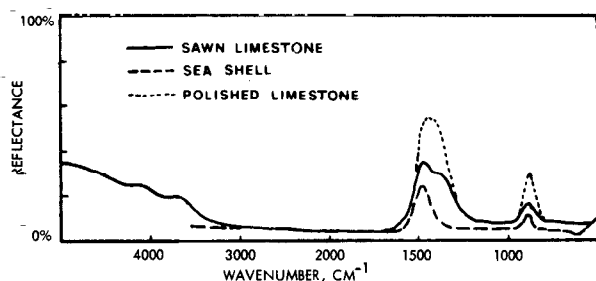


FIG. 14. Reflectance spectra of a clam-like sea shell exterior and limestone sawn and polished showing the  $\text{CaCO}_3$  similarity in each.

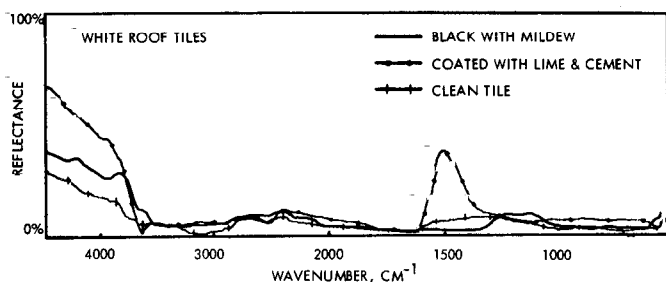


FIG. 15. Reflectance of roof tiles used in Florida to reduce solar energy heating: clean white tile; tile black with mildew, and tile coated with a mixture of white lime and white cement. The  $\text{CaCO}_3$  influence of the lime is seen. All three show the desired high emittance (low reflectance) to maximize loss of heat by radiation.

absorber surface which McDonald<sup>11</sup> has reported to be a good collector. The "Martin Black" surface shown is amazingly black in the visible and quite diffuse, but it can be seen that it does not have the desired solar selective properties. Hundreds of samples have already

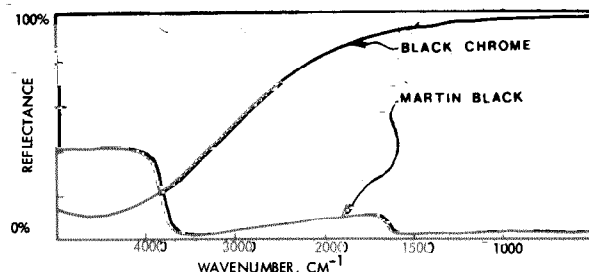


FIG. 16. Black chrome solar selective surface to minimize radiative heat loss due to its low emittance (high reflectance). Martin Black shows a velvet black appearance in the visible, and is seen to be of high emittance in the ir except toward the near ir.

been measured by this instrument in the development of solar collector coatings.

### III. SUMMARY

It is now practical to measure the reflectance or emittance of most materials at ambient temperature, or even at elevated or reduced temperatures. The Willey 318 spectrophotometer with diffuse reflectance (integrating sphere) module has made these measurements routine. Properties of materials that were otherwise difficult if not impossible to measure are now easily obtained. Essentially all of the conventional transmittance ir capabilities are retained, and the data manipulation capabilities have been added.

We believe that a new dimension has been added to ir spectrophotometry.

1. N. J. Harrick, *Internal Reflection Spectroscopy* (Wiley, New York, 1967), p. 30.
2. R. W. Frei and J. D. MacNeil, *Diffuse Reflectance Spectroscopy in Environmental Problem-Solving* (CRC Press, Cleveland, 1973), pp. 3, 209.
3. A. C. Hardy, *J. Opt. Soc. Am.* 25, 305 (1935).
4. W. W. Coblenz, *Investigations of Infra-Red Spectra* (Carnegie Institute of Washington, Oct. 1905, No. 35, Reprinted 1962 by the Coblenz Society), Parts IV and V.
5. W. A. Hovis, Jr. and W. R. Callahan, *J. Opt. Soc. Am.* 56, 639 (1966).
6. M. J. D. Low, *Appl. Opt.* 6, 1503 (1967).
7. S. T. Dunn, J. C. Richmond, and J. F. Farmer, *J. Spacecraft Rockets* 3, 961, (1966) (Reprinted in NBS Spec. Publ. 300, Vol. 7).
8. J. C. Richmond and W. N. Harrison, *Am. Ceramic Soc. Bull.* 39, 668 (1960) (Reprinted in NBS Spec. Publ. 300, Vol. 7).
9. H. B. Curtis, *J. Spacecraft* 3, 383 (1966).
10. J. T. Geir, R. V. Dunkle, and J. T. Bevans, *J. Opt. Soc. Am.* 44, 558 (1954).
11. J. U. White, *J. Opt. Soc. Am.* 54, 1332 (1964).
12. H. H. Keegan and V. R. Weidner, *J. Opt. Soc. Am.* 56, 523, 56, 1453A, 56, 540A (1966).
13. A. C. Hardy and F. H. Perrin, *The Principles of Optics* (McGraw-Hill, New York, 1932), p. 280.
14. H. Sakai, *Aspen International Conference On Fourier Spectroscopy* (1970), AFCRL-71-0019, Special Reports No. 114, (5 Jan. 1971), p. 19.
15. G. A. Vanasse and H. Sakai, *Progress In Optics*, E. Wolf, Ed. (North-Holland, Amsterdam, 1967) Vol. VI, p. 284.
16. L. Mertz, *Transformations In Optics* (Wiley, New York, 1965), p. 20ff, p. 42.
17. J. Connes, *Aspen International Conference On Fourier Spectroscopy* (1970), AFCRL-71-0019, Special Reports No. 114, (5 Jan. 1971), p. 83.
18. R. S. Hernicz and D. P. DeWitt, *Appl. Opt.* 12, 2454 (1973).
19. J. R. Aronson and A. G. Emslie, *Appl. Opt.* 12, 2563 (1973).
20. M. R. Querry, R. C. Waring, W. E. Holland, L. M. Earls, M. D. Herrman, W. P. Nijm and G. M. Hale, *J. Opt. Soc. Am.* 64, 39 (1974).
21. G. E. McDonald, *NASA Technical Memorandum NASA TM X-3136* (Dec. 1974).